Smart Structures and Systems, *Vol. 25, No. 5 (2020) 559-567*
DOI: https://doi.org/10.12989/sss.2020.25.5.559

Multiple model switching adaptive control for vibration control of cantilever beam with varying load using MFC actuators and sensors

Zhiyuan Gao, Jiaqi Huang, Zhonghua Miao and Xiaojin Zhu*

School of Mechatronic Engineering and Automation, *Shanghai University*, *No. 333 Nanchen Road*, *Shanghai*, *P.R. China*

(*Received July 19, 2019, Revised November 21, 2019, Accepted December 24, 2019*)

Abstract. Vibration at the tip of various flexible manipulators may affect their operation accuracy and work efficiency. To suppress such vibrations, the feasibility of using MFC actuators and sensors is investigated in this paper. Considering the convergence of the famous filtered-x least mean square (FXLMS) algorithm could not be guaranteed while it is employed for vibration suppression of plants with varying secondary path, this paper proposes a new multiple model switching adaptive control algorithm to implement the real time active vibration suppression tests with a new multiple switching strategy. The new switching strategy is based on a cost function with reconstructed error signal and disturbance signal instead of the error signal from the error sensor. And from a robustness perspective, a new variable step-size sign algorithm (VSSA) based FXLMS algorithm is proposed to improve the convergence rate. A cantilever beam with varying tip mass is employed as flexible manipulator model. MFC layers are attached on both sides of it as sensors and actuators. A co-simulation platform was built using ADAMS and MATLAB to test the feasibility of the proposed algorithms. And an experimental platform was constructed to verify the effectiveness of MFC actuators and sensors and the real-time vibration control performance. Simulation and experiment results show that the proposed FXLMS algorithm based multiple model adaptive control approach has good convergence performance under varying load conditions for the flexible cantilever beam, and the proposed FX-VSSA-LMS algorithm based multiple model adaptive control algorithm has the best vibration suppression performance.

Keywords: active vibration control; MFC actuators and sensors; adaptive control; multiple model switching

1. Introduction

Flexible mechanical arms made by flexible components have been widely used in the fields of high-precision industry and aerospace industry in recent years (Kiang *et al*. 2015). However, the vibration at the end of the flexible robot arms with varying loads may affect the operation accuracy and work efficiency (Ma *et al*. 2015). Structural vibration control should be concerned due to numerous reasons, including but not limited to fatigue-induced failure, excessive wearing of machinery, and radiated noise. Conventional passive vibration suppression methods are unsuitable for such applications while less weight is desired and low frequency vibration should be suppressed. In this era, there is a growing interest towards smart materials in order to achieve sensing and actuation. Piezoelectric materials are a class of smart materials which are often used in energy harvesting, vibration control, and health monitoring applications as they exhibit strong electro-mechanical coupling, large blocking force, high structural stiffness and quick response time. But due to its high brittleness, low flexibility and low conformity to curved surfaces, its applications are limited (Song *et al*. 2006, Gripp and Rade 2018).

To overcome these limitations, NASA developed Macro fiber composite (MFC) which have piezoelectric fibers with rectangular cross section surrounded by polymer matrix and sandwiched between protective and electrode layers. The feasibility of using MFC actuators and sensors to suppress circular plate vibration is investigated by Leniowska and Mazan (2015). Actuation equation of MFC coupled plate in different boundary conditions is deduced, and an equivalent finite element modeling method is proposed which uses MFC actuating force as the applied excitation by Tu *et al*. (2018). To give an accurate prediction of MFC bonded smart structures for the simulation of shape and vibration control, a linear electro-mechanically coupled static and dynamic finite element models based on the first-order shear deformation hypothesis is developed by Zhang *et al*. (2017).

In order to generate a proper anti-disturbance signals for the actuators of various smart structures, many control algorithms have been proposed. Among these algorithms, FXLMS algorithm becomes the most popular adaptive feedforward control method with simple structure, and fast convergence properties (Morgan 2013). Ardekani analyzed the convergence of FXLMS algorithm theoretically (Ardekani and Abdulla 2010). Leva implemented FXLMS algorithm based vibration controller using a high-speed computational architecture, based on a field programmable

*Corresponding author, Ph.D., Professor,
E-mail: mgzhuxj@shu.edu.cn

http://www.techno-press.org/?journal=sss&subpage=7

ISSN: 1738-1584 (Print), 1738-1991 (Online)

gate array (Leva and Piroddi 2011). Huang implemented an improved multi-input multi-output filtered-X least mean square algorithm (Huang *et al*. 2013).

But if we implemented FXLMS algorithm for active vibration control of flexible mechanical arms with varying loads, the convergence of the algorithm will decrease, or even worse, controller would diverge. Online system identification techniques are required to ensure the convergence of the FXLMS algorithm. Many researchers have made considerable efforts to develop FXLMS with online identification strategy for practical purposes. A new ononarc-tangent function based FX-VSSLMS algorithm improving the convergence compared with conventional FXLMS is proposed by Gomathi and Saravanan (2016). A new multi-channel FXLMS with online secondary path modelling based on the auxiliary random noise technique is proposed by Pu *et al*. (2019). An enhanced FXLMS algorithm using simultaneous equation method for adaptive vibration suppression of time-varying structures is proposed by Niu *et al*. (2019). While if the models of the controlled plant with different loads could be identified offline which is more practical for flexible manipulators, multiple model switching strategies may also be a better choice.

Zhao investigated self-organizing map based multi-model inverse control algorithms can improve the control performance of the investigated system, as compared with the classical PD controller (Zhao *et al*. 2016), and it shows multiple model strategy may be a good choice for active noise control or active vibration control applications. Zhao set up multiple models to cover the uncertainty of the real secondary path to deal with a grand uncertain secondary path problem in active noise control (Zhao *et al*. 2007). Huang proposed a multiple model switching based active noise control algorithm and implemented on Texas Instruments digital signal processor (DSP) TMS320F28335 and real time experiments were done to show the effectiveness of using multiple model strategy (Huang *et al*. 2017).

Considering the multiple model switching strategy proposed in Huang *et al*. (2017) has an white noise excitation input, which is also a disturbance for the vibration control system, this paper proposes a new multiple model switching strategy with a new cost function by reconstructing the error and the disturbance signal. The computation burden of the proposed multiple model switching strategy could be significantly reduced as none online adaptive model identification process is carried out. And more, to improve the convergence of FXLMS algorithm, a variable step-size sign algorithm proposed by Li *et al*. (2014) is employed to deduce a new FX-VSSA-LMS based multiple model adaptive control algorithm.

In this paper, six Macro Fiber Composite (MFC) patches are applied for vibration sensing and active control for a cantilever beam. Four of them are utilized as actuators: Two provides the excitation force, the others create the control force. Two of them are used as sensors. Model sets of different secondary paths are established for a piezoelectric flexible beam with different tip mass using offline system identification. Whenever the load of the cantilever beam changes, an optimal controller based on FXLMS or FX-VSSA-LMS algorithm with the corresponding secondary path model could be selected to achieve a good vibration suppression performance according to our proposed model switching criterion. Utilizing the proposed control algorithm, the active vibration control of the first three vibration modes is implemented. The effectiveness of the MFC sensor and actuator for sensing and controlling vibration is validated by experiment. And the feasibility of the proposed two multiple model adaptive control algorithms are also validated by both simulation and experiment.

2. Constitutive relationships of MFCs

Thin piezoelectric actuators and sensors are used in a variety of applications such as active vibration control, structural health monitoring or shape control. In these applications, PZT ceramics are commonly used due to their relatively low cost, high bandwidth and good actuation capabilities. The major drawbacks of these ceramics are their brittleness and very low flexibility. This problem can be overcome using piezocomposite transducers in which piezoelectric fibers are mixed with a softer passive epoxy matrix. A typical piezocomposite transducer is made of an active layer sandwiched between two soft thin encapsulating layers as shown in Fig. 1 (Deraemaeker and Nasser 2010). In terms of practical applications, Macro Fiber Composite (MFC) piezoelectric sensors/actuators are particularly interesting. They are laminated structures with built-in piezoelectric fibers and electrodes enabling the use of the piezoelectric effect. MFC elements offer many advantages: they have low weight and rigidity; they can be assembled in a laminate; they are resistant to elevated temperatures occurring in the laminate production process. Schematic representation of d33 and d31 type MFC is shown in Fig. 2.

For d33-MFCs, using the standard IEEE notations for linear piezoelectricity, the constitutive equations for an orthotropic piezoelectric material are given by Eq. (1).

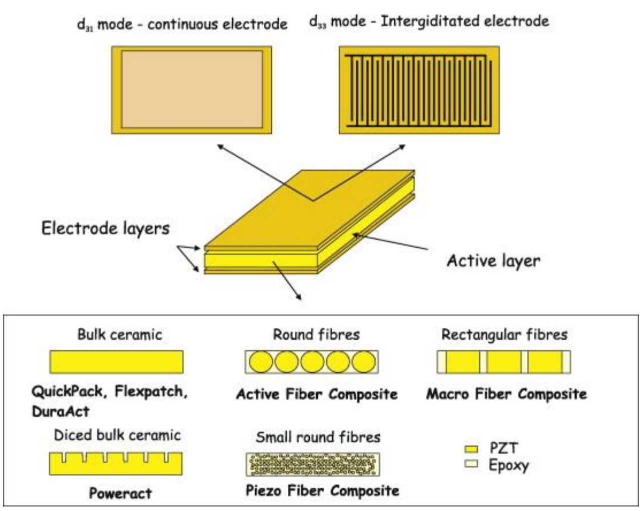

Fig. 1 Flat piezocomposite transducers with surface electrodes (Deraemaeker and Nasser 2010)

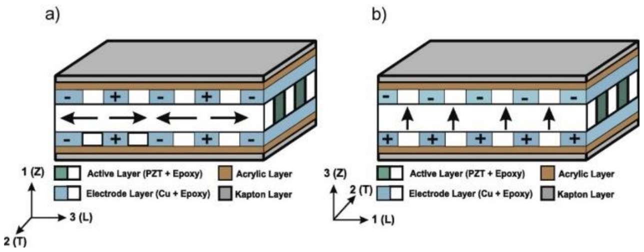

Fig. 2 Schematic representation of d33 and d31 type MFC (Pandey and Arockiarajan 2017)

$$\begin{Bmatrix} T_1 \\ T_2 \\ T_3 \\ T_4 \\ T_5 \\ T_6 \\ D_1 \\ D_2 \\ D_3 \end{Bmatrix} = \begin{bmatrix} c_{11}^E & c_{12}^E & c_{13}^E & 0 & 0 & 0 & 0 & 0 & -e_{31} \\ c_{12}^E & c_{22}^E & c_{23}^E & 0 & 0 & 0 & 0 & 0 & -e_{32} \\ c_{13}^E & c_{23}^E & c_{33}^E & 0 & 0 & 0 & 0 & 0 & -e_{33} \\ 0 & 0 & 0 & c_{44}^E & 0 & 0 & 0 & -e_{24} & 0 \\ 0 & 0 & 0 & 0 & c_{55}^E & 0 & -e_{15} & 0 & 0 \\ 0 & 0 & 0 & 0 & 0 & c_{66}^E & 0 & 0 & 0 \\ 0 & 0 & 0 & 0 & e_{15} & 0 & \varepsilon_{11}^S & 0 & 0 \\ 0 & 0 & 0 & e_{24} & 0 & 0 & 0 & \varepsilon_{22}^S & 0 \\ e_{31} & e_{32} & e_{33} & 0 & 0 & 0 & 0 & 0 & \varepsilon_{33}^S \end{bmatrix} \begin{Bmatrix} S_1 \\ S_2 \\ S_3 \\ S_4 \\ S_5 \\ S_6 \\ E_1 \\ E_2 \\ E_3 \end{Bmatrix} \tag{1}$$

Here E_i and D_i are the components of the electric field vector and the electric displacement vector, and T_i and S_i are the components of stress and strain vectors.

For d33 piezocomposites, the plane stress hypothesis implies that $T_1 = 0$. The constitutive equations are given by Eq. (2).

$$\begin{Bmatrix} T_2 \\ T_3 \\ T_4 \\ T_5 \\ T_6 \\ D_3 \end{Bmatrix} = \begin{bmatrix} c_{22}^{E*} & c_{23}^{E*} & 0 & 0 & 0 & -e_{31}^* \\ c_{23}^{E*} & c_{33}^{E*} & 0 & 0 & 0 & -e_{32}^* \\ 0 & 0 & c_{44}^{E*} & 0 & 0 & 0 \\ 0 & 0 & 0 & c_{55}^{E*} & 0 & 0 \\ 0 & 0 & 0 & 0 & c_{66}^{E*} & 0 \\ e_{31}^* & e_{32}^* & 0 & 0 & 0 & \varepsilon_{33}^{S*} \end{bmatrix} \begin{Bmatrix} S_1 \\ S_2 \\ S_4 \\ S_5 \\ S_6 \\ E_3 \end{Bmatrix} \tag{2}$$

3. FXLMS and FX-VSSA-LMS algorithm

3.1 FXLMS algorithm

In terms of adaptive control algorithms, myriad methods have been implemented in vibration suppression. Among them, the adaptive filtered-x least mean square (FXLMS) algorithm has wide applications due to its simplicity and robustness for active noise control and vibration control applications. Block diagram of the classical FXLMS algorithm based on the gradient descent method is illustrated in Fig. 3.

In Fig. 3, $x(n)$ is the external disturbance that usually serves as the feedforward reference signal, where n indicates the time sequence; $P(z)$ is the open-loop response of the primary path under vibration disturbance excitation; $S(z)$ is the secondary path to generate response $y'(n)$ to cancel $d(n)$; the residual vibration response $e(n)$ is the superposition of $d(n)$ and $y'(n)$; $W(z)$ is the finite impulse response filter and its coefficients are adaptively updated to control the secondary path $S(z)$ for minimum $e(n)$ in real-time; the coefficient updates are ruled by least mean square (LMS) algorithm whose inputs are filtered reference signal $x'(n)$ and residual response $e(n)$; $x'(n)$ refers to $x(n)$ filtered by the offline-estimated secondary path.

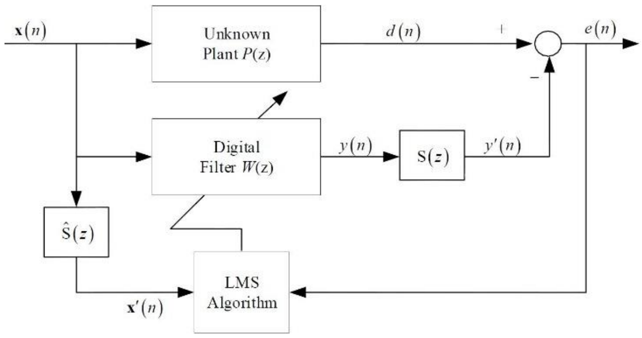

Fig. 3 Block diagram of classical FXLMS algorithm

The output of the FXLMS controller is

$$y(n) = \boldsymbol{X}^T(n) * W(n) \tag{3}$$

The update equation for the coefficients of $W(z)$ is

$$W(n+1) = W(n) + \mu e(n)\boldsymbol{X}'(n) \tag{4}$$

Here, $\boldsymbol{X}'(\boldsymbol{n})$is the reference signal $\mathbf{x}(n)$ filtered by the estimated secondary path model$\hat{S}(z)$. In FXLMS algorithm, μ is the step factor, and

$$0 < \mu < 1/\lambda_{max} \tag{5}$$

Here, λ_{max} is the largest eigenvalue of the input signal variance matrix.

3.2 FX-VSSA-LMS algorithm

While a vibration control system employs the above FXLMS algorithm, the convergence speed would affect the stability of the vibration controller. Variable step-size (VSS) techniques could be adopted in the least-mean-square (LMS) algorithm for improving the convergence rate. Among them, Li proposes a new variable step-size sign algorithm (VSSA) for unknown channel estimation or system identification, and applies this algorithm to an environment containing two-component Gaussian mixture observation noise (Li *et al.* 2014). The step size is adjusted using the gradient-based weighted average of the sign algorithm. The proposed scheme exhibits a fast convergence rate and low misadjustment error, and provides robustness in environments with heavy-tailed impulsive interference. In this paper, we adopted this VSSA algorithm to develop a new type FX-VSSA-LMS algorithm. The block diagram of the proposed FX-VSSA-LMS algorithm is shown in Fig. 4.

The update equations of the step size is shown as follows

$$\begin{aligned} \mu(n) &= a\mu(n-1) + \gamma||p(n)||^2 \\ p(n) &= \lambda p(n-1) + (1-\lambda)sign(e(n))x(n) \end{aligned} \tag{6}$$

Similar to the step size, the parameter γ determines the convergence time and level of misadjustment of the

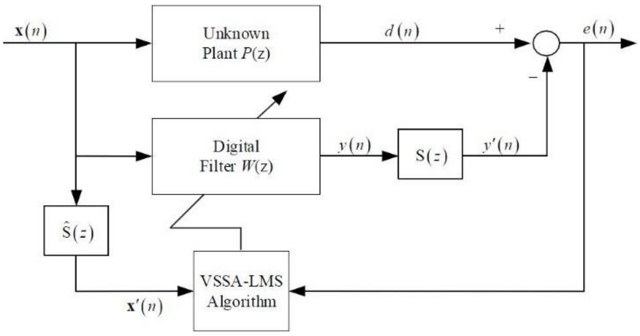

Fig. 4 Block diagram of the proposed FX-VSSA-LMS algorithm

algorithm.

The output of FX-VSSA-LMS controller is

$$y(n) = \boldsymbol{X}^T(n) * W(n) \tag{7}$$

The update equation for the coefficients of $W(z)$ is

$$W(n+1) = W(n) + \mu(n)e(n)\boldsymbol{X}'(n) \tag{8}$$

4. The proposed multiple model adaptive control algorithm

4.1 FXLMS algorithm based multi-model switching adaptive control

Multi-model switching adaptive control structure is mainly composed of three parts: identification model set, switching criterion, and controller set. Fig. 5 shows FXLMS algorithm based multi-model switching adaptive control using the multi-model switching strategy proposed in Huang *et al*. (2017).

Here $S_1(z)$,$S_2(z)$,…,$S_m(z)$ are secondary path models of the identification model set. $\hat{S}_s(z)$ is the secondary path model selected by switching criterion using residual test. $m(n)$ is a zero-mean white noise used to drive the secondary path models. When the secondary path changes rapidly, the multi-model switching criterion could detect the change and switch to the appropriate secondary path model $\hat{S}_s(z)$ with the minimum cost function shown in Eq. (9)

$$\boldsymbol{J_i(n)} = \sum_{\boldsymbol{j=0}}^{\boldsymbol{n}} \boldsymbol{e^{-\lambda(n-j)}\varepsilon_i^2(j)} \tag{9}$$

Here $\varepsilon_i(n)$ is the residual error for the i-th model

$$\varepsilon_i(n) = e(n) - y_i(n) \tag{10}$$

λ is forgetting factor, *t* is time index. The model which has the minimum residual power is selected as current $\hat{S}_s(z)$.

4.2 New FXLMS algorithm based multi-model switching adaptive control

Considering the switching criterion proposed in Huang *et al*. (2017) has a white noise input, which is also a disturbance for the control system, this paper proposes a new multiple model switching criterion with new cost function using reconstructing the error and the disturbance signal as shown in Fig. 6.

As shown in Fig. 6, signal reconstruction technique is employed in the proposed algorithm by using the identified secondary path model set. And $e_{r1}(n), e_{r2}(n), \cdots, e_{rm}(n)$ is the reconstructed error signal and $d_{r1}(n)$, $d_{r2}(n)$, $\cdots$, $d_{rm}(n)$ is the reconstructed disturbance signal. The cost function $J_i(n)$ can be improved using the reconstructed error signal $e_{ri}(n)$ and the reconstructed disturbance signal $d_{ri}(n)$.

$$J_i(n) = \frac{\alpha_e\|e_{ri}(n)\|^2 + \beta_e \sum_{j=0}^{n-1} e^{-\lambda_e(n-j)}\|e_{ri}(j)\|^2}{\alpha_d\|e_{ri}(n)\|^2 + \beta_d \sum_{j=0}^{n-1} e^{-\lambda_d(n-j)}\|e_{ri}(j)\|^2} \tag{11}$$

Here α_e and α_d are the weighting factors for the current reconstructed error signal and the reconstructed

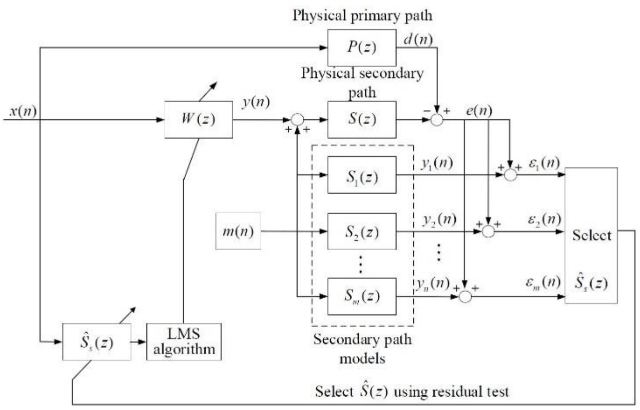

Fig. 5 Block diagram of multiple model adaptive control structure

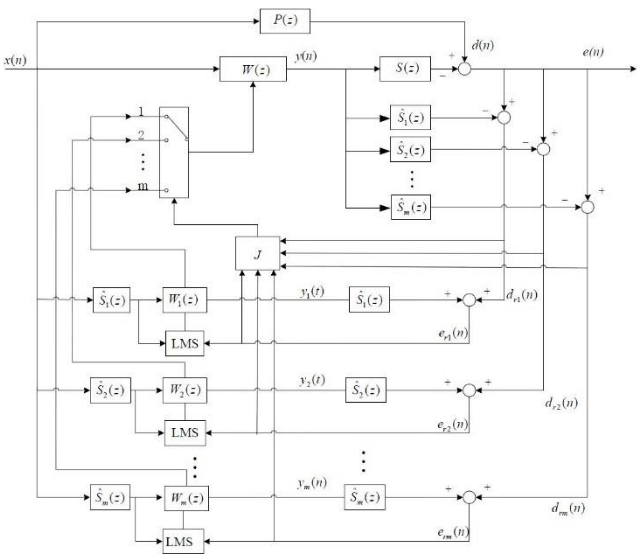

Fig. 6 Block diagram of FXLMS algorithm based multi-model switching adaptive control

disturbance signal. β_e and β_d are the weighting factors for the past reconstructed error signal and the reconstructed disturbance signal. λ_e and λ_d are the forgetting factors which could guarantee the cost function bounded. If larger $\frac{\alpha_e}{\beta_e}$, $\frac{\alpha_d}{\beta_d}$, λ_e and λ_d are chosen for the cost function, faster response time could be expected but with more mis-switchings. While smaller $\frac{\alpha_e}{\beta_e}$, $\frac{\alpha_d}{\beta_d}$, λ_e and λ_d are chosen for the cost function, response time will be extended.

The algorithm procedure can be shown as follows:

(1) Constructing a model bank with m fixed secondary path models;
(2) Calculating $J_i(n)$ for each model;
(3) Selecting $\hat{S}_s(z)$ which has the minimum residual power;
(4) Employing the FxLMS controller corresponding to the selected $\hat{S}_s(z)$. The computation burden of the proposed multiple model switching strategy could be significantly reduced as none online adaptive model identification is carried out.

4.3 New FX-VSSA-LMS algorithm based multi-model switching adaptive control

The VSSA algorithm in section 3.2 combines the benefits of the gradient-based algorithm and sign algorithm. The gradient-based algorithm makes the proposed algorithm converge fast with colored input signals and simultaneously the sign algorithm guarantees its robustness against impulsive interference. By adopting VSSA into the proposed FXLMS algorithm based multi-model switching adaptive control in section 4.2, a new type FX-VSSA-LMS algorithm based multi-model switching adaptive control approach is shown in Fig. 7.

For easy understanding of the proposed algorithm, the algorithm procedure of the proposed FX-VSSA-LMS algorithm based multi-model switching adaptive control algorithm is summarized as follows:

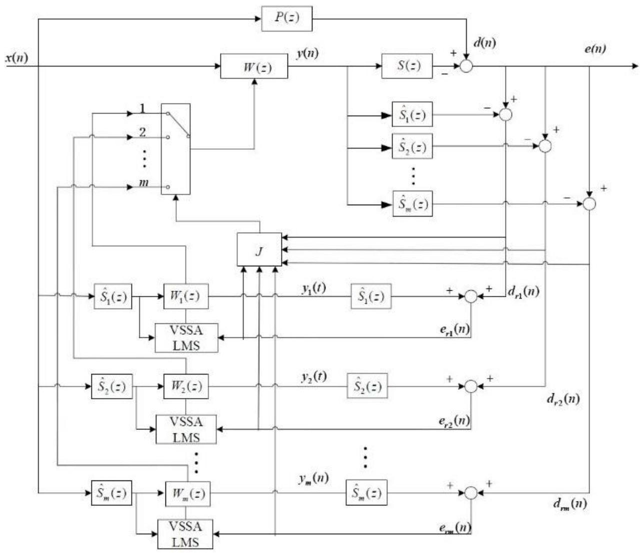

Fig. 7 Block diagram of FX-VSSA-LMS algorithm based multi-model switching adaptive control

(1) Constructing a model bank with m fixed secondary path models;
(2) Calculating $J_i(n)$ for each model using Eq. (11);
(3) Selecting $\hat{S}_s(z)$ which has the minimum residual power;
(4) Employing the FX-VSSA-LMS controller corresponding to the selected $\hat{S}_s(z)$.

5. Co-simulation with Adams and Simulink

A cantilever beam with varying tip mass can be employed as a test benchmark for flexible manipulators with varying loads. To test the feasibility of the proposed algorithm, a co-simulation platform was built using ADAMS and MATLAB Simulink. MFC layers are attached on the both sides of a cantilever beam as sensors and actuators to construct a smart beam. The structural diagram of the flexible cantilever beam with varying load is shown in Fig. 8. The length of the cantilever beam is 500 mm. The width of the cantilever beam is 35 mm. The thickness of the cantilever beam is 1 mm. The elasticity modulus of the cantilever beam is 190 GPa. The density of the cantilever beam is 8 g/cm^3. The Poisson's ratio of the cantilever beam is 0.29. The weight of the cantilever beam is 140 g.

The virtual prototype built in Adams is mainly divided into three parts, as shown in Fig. 9. Part 1 is a fixed base, part 2 is the flexible cantilever beam with MFC layers attached on the both sides as sensors and actuators, and part 3 is a mass block which could be varied from 0 g to 140 g.

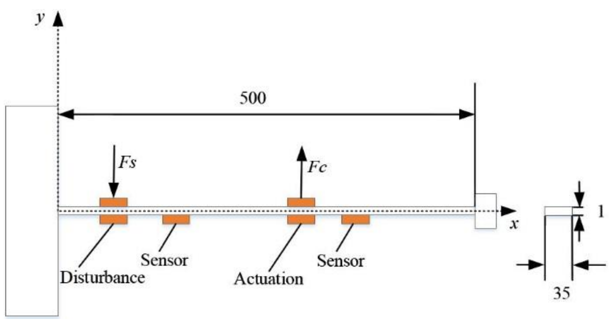

Fig. 8 Structural diagram of flexible cantilever beam with varying load

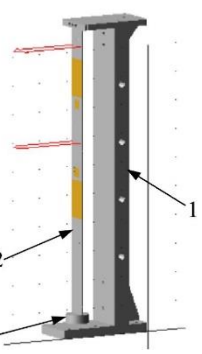

Fig. 9 Virtual prototype of the smart cantilever beam with varying tip mass

Frequency characteristics of the secondary path for the whole system under different operating loads is shown in Fig. 10. Model 0 is the secondary path model with empty loads. Model 1 is the secondary path model with 14 g loads. Model 2 is the secondary path model with 28 g loads. Model 3 is the secondary path model with 42 g loads. Model 4 is the secondary path model with 56 g loads. Model 5 is the secondary path model with 70 g loads. Model 6 is the secondary path model with 84 g loads. Model 7 is the secondary path model with 98 g loads. Model 8 is the secondary path model with 112 g loads. Model 9 is the secondary path model with 126 g loads. Model 10 is the secondary path model with 140 g loads.

Data communication unit of Adams and MATLAB is shown in Fig. 11. These modules could be imported into Simulink to establish a co-simulation program.

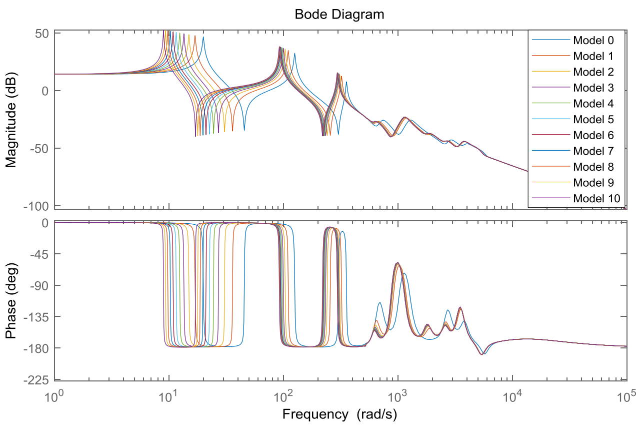

Fig. 10 Frequency characteristics under different loads

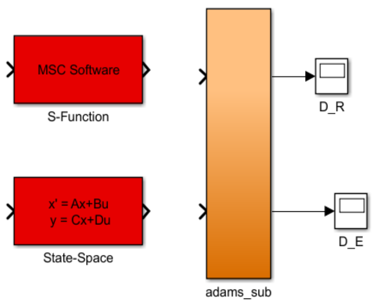

Fig. 11 Data communication unit of Adams and MATLAB

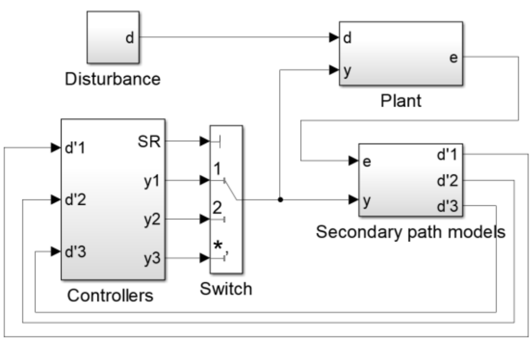

Fig. 12 Co-simulation Simulink program for multiple model adaptive control

The co-simulation Simulink program for multiple model adaptive control is shown in Fig. 12.

Comparison simulations are done to test the feasibility and advantages of the proposed FXLMS algorithm based multi-model switching adaptive control algorithm, as well as the proposed FX-VSSA-LMS algorithm based multi-model switching adaptive control algorithm. And FXLMS algorithm with online secondary path modelling method proposed by Pu *et al.* (2019) is also compared to show the advantages of the proposed algorithms.

To compare the control performance of different control algorithms, a narrowband signal combined by the first three natural frequencies of Model 0, Model 1 and Model 5 is employed as the vibration disturbance signal. The tip mass is 0 g from 0 s to 40 s. The tip mass is 14 g from 40 s to 80 s. While the tip mass is 70 g from 80 s to 120 s.

As it is shown in Fig. 13, algorithm A is FXLMS algorithm with online secondary path modelling method proposed by Pu *et al.* (2019), algorithm B is the FXLMS algorithm with multiple model switching stategy proposed by Huang *et al.* (2017), algorithm C is our proposed FXLMS algorithm based multi-model switching adaptive control algorithm, and algorithm D is our proposed FX-VSSA-LMS algorithm based multi-model switching adaptive control algorithm.

With the same FXLMS controller and the same initial condition, the proposed multiple model switching adaptive control algorithm could provide a better vibration suppression performance. While the vibration control performance of the proposed FX-VSSA-LMS algorithm based multi-model switching adaptive control algorithm is much better than traditional FXLMS algorithm based multi-model switching adaptive control algorithm.

To compare the control performance, a control performance index (CPI) is defined as follows

$$CPI = 20\,log_{10}\frac{\sum_{i=1}^{N}|e(i)|^2}{\sum_{i=1}^{N}|d(i)|^2} \tag{12}$$

$d(i)$ is the output of the error sensor without active vibration control. And $e(i)$ is the output of the error sensor under active vibration control. While the vibration disturbance is suppressed, CPI is negative. While the active

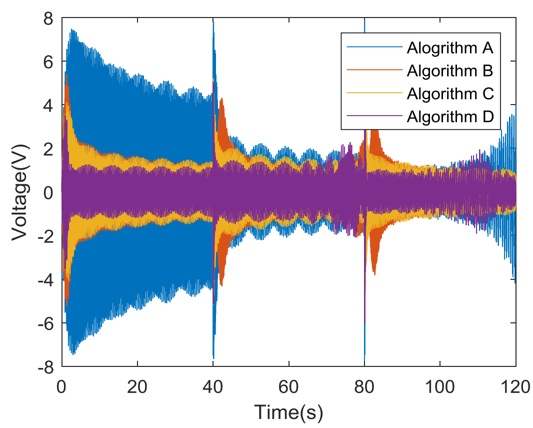

Fig. 13 Co-simulation control performance comparison

vibration controller failed to suppress the vibration disturbance, CPI is positive.

The CPI of FXLMS with with online secondary path modelling method proposed by Pu *et al*. (2019) is -16.35 dB. The CPI of our proposed FXLMS algorithm based multi-model switching adaptive control algorithm is -51.53 dB. While under the same condition, the CPI of the algorithm proposed in Huang *et al*. (2017) is -43.92 dB, which also confirms the good vibration suppression performance of our proposed algorithm. The CPI of our proposed FX-VSSA-LMS algorithm based multi-model switching adaptive control algorithm is -64.67 dB, which is best CPI among these algorithms. And it confirms the feasibility and advantages of the proposed multiple model switching strategy and the two improved algorithms.

6. Experimental results and analysis

The schematic diagram and experimental configuration of the real time experimental platform are illustrated in Fig. 14. A stainless steel beam with a tip mass is employed to simulate flexible robot arm with varying loads. To suppress the vibration response while the beam is subjected to continuous excitations, MFC actuators and sensors are attached to the surface of the beam to construct a smart piezoelectric beam. The type of the MFC actuator is M-5628-P2. The length of each actuator is 56 mm, and the width is 28 mm. The driving voltage range is 0-300V. The type of the MFC sensor is M-0714-P2. The length of each sensor is 14 mm, and the width is 7 mm.

A Matlab XPC real time control system is established using two charge amplifiers (YE5852A made by Sinocera Piezotronics, Inc.), a four channel power amplifier (E01.A4 made by CoreMorrow), and an NI PCI-6289 data acquisition board. The input voltage range of the power amplifier is 0-10 V, and amplification factor is 30. The average power of each channel is 35 W, and the ripple is 5 mV. The charge input range of the charge amplifier is $\pm 10^6$ pC, and the output voltage range of the charge amplifier is ± 10 V. The output noise is less than 5 μV.

The photograph of the experimental platform is shown in Fig. 15. In addition, all of the control algorithms are developed with Matlab Simulink.

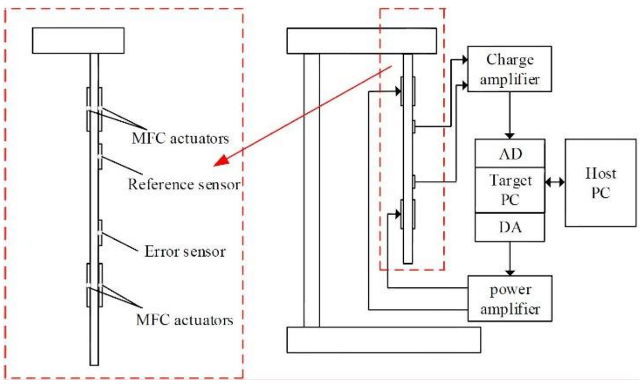

Fig. 14 Schematic diagram and experimental configuration of the experimental platform

To evaluate the effectiveness of the proposed controller, firstly, a vibration disturbance is imposed on the beam surface. And the vibration response of the vibrating beam is obtained by the piezoelectric MFC sensor attached on flexible beam. Then the electric charge signal of the piezoelectric MFC sensor is changed to voltage signal by the charge amplifier. After A/D conversion, the collected digital signals are obtained by the target PC. Based on Matlab XPC environment, the control signal is calculated according to the four algorithms in section 5. Then the digital control signal is input into the power amplifier after D/A conversion. Finally, the amplified control signal is imposed on the piezoelectric MFC actuator to suppress the vibration of the flexible beam.

Narrowband signal combined by the first three natural frequencies of the smart cantilever beam with 0 g tip mass, 14 g tip mass and 68 g tip mass is employed as the vibration disturbance signal. Real time control experiments are done to verify the real-time control performance. The tip mass is 0 g from 0 s to 40 s. The tip mass is 14 g from 40 s to 80 s. While the tip mass is 68 g from 80 s to 120 s. There are two methods to change the tip mass: (1) Using neodymium magnets to change the tip mass without stopping the real time control experiment, and the weight of each neodymium magnet is 1 g. (2) Assembling different stainless steel discs from 14 g to 140 g, and restart a new real time control experiment.

As shown in Fig. 16, algorithm A is FXLMS algorithm with online secondary path modelling method proposed by Pu *et al*. (2019), algorithm B is the FXLMS algorithm with multiple model switching strategy proposed by Huang *et al*.

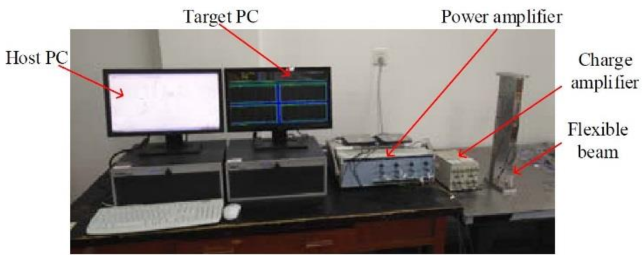

Fig. 15 Schematic diagram and experimental configuration of the experimental platform

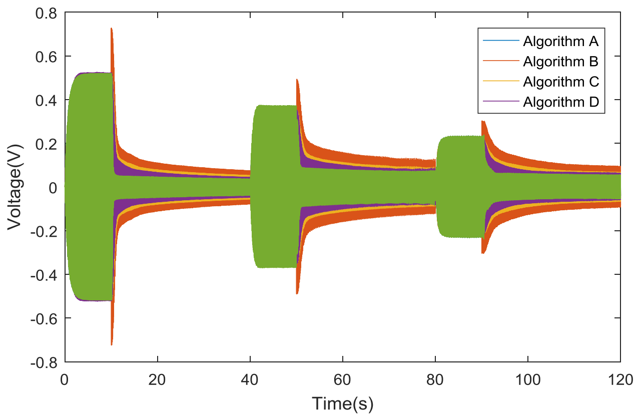

Fig. 16 Real time control performance comparison

(2017), algorithm C is our proposed FXLMS algorithm based multi-model switching adaptive control algorithm, and algorithm D is our proposed FX-VSSA-LMS algorithm based multi-model switching adaptive control algorithm. The CPI of algorithm A is -47.38 dB. The CPI of algorithm B is -60.83 dB. The CPI of algorithm C is -65.32 dB. The CPI of algorithm D -77.73 dB. And it confirms the feasibility and advantages of the proposed multiple model switching strategy and the two improved algorithms again. Experimental results show that the proposed FXLMS algorithm based multiple model adaptive control approach has better convergence performance under varying load conditions for the flexible cantilever beam comparing with the FXLMS algorithm with online secondary path modelling, and the proposed FX-VSSA-LMS algorithm based multiple model adaptive control algorithm has the best vibration suppression performance.

7. Conclusions

The feasibility of using MFC actuators and sensors to suppress the vibration at the tip of various flexible manipulators is investigated in this paper. Two new multi-model switching adaptive control algorithms were proposed to ensure that the optimal controller is matched to control the flexible cantilever beam when the load of the beam changes. The computation burden of the proposed multiple model switching strategy is significantly reduced as none online adaptive model identification is carried out. The proposed algorithms are tested and compared on an Adams and Matlab Simulink co-simulation platform. Preliminary simulation results show the proposed two algorithms are effective with good transient performance. A stainless steel beam with a tip mass is employed to simulate flexible robot arm with varying loads. Six Macro Fiber Composite (MFC) patches are applied for vibration sensing and active control for a cantilever beam. Four of them are utilized as actuators: Two provides the excitation force, the others create the control force. Two of them are used as a sensor. The real time experimental results verify that the proposed multiple model switching adaptive vibration control system using MFC actuators and sensors can be employed to suppress the tip vibration flexible manipulators.

Acknowledgments

The research described in this paper was financially supported by the National Natural Science Foundation of China (Grant Nos. 51575328, 61503232), “Chen Guang” project supported by Shanghai Municipal Education Commission and Shanghai Education Development Foundation (No. 15CG44).

References

Ardekani, I.T. and Abdulla, W.H. (2010), “Theoretical convergence analysis of FxLMS algorithm”, *Signal Process.*, **90**(12), 3046-3055. https://doi.org/10.1016/j.sigpro.2010.05.009

Deraemaeker, A. and Nasser, H. (2010), “Numerical evaluation of the equivalent properties of Macro Fiber Composite (MFC) transducers using periodic homogenization”, *Int. J. Solids Struct.*, **47**(24), 3272-3285. https://doi.org/10.1016/j.ijsolstr.2010.08.006

Gomathi, K. and Saravanan, V. (2016), “Variable step size for improving convergence of FxLMS algorithm”, *Procedia Technol.*, **25**, 420-426. https://doi.org/10.1016/j.protcy.2016.08.127

Gripp, J. and Rade, D. (2018), “Vibration and noise control using shunted piezoelectric transducers: a review”, *Mech. Syst. Signal Process.*, **112**, 359-383. https://doi.org/10.1016/j.ymssp.2018.04.041

Huang, Q., Zhu, X., Gao, Z., Gao, S. and Jiang, E. (2013), “Analysis and implementation of improved multi-input multi-output filtered-X least mean square algorithm for active structural vibration control”, *Struct. Control Health Monitor.*, **20**(11), 1351-1365. https://doi.org/10.1002/stc.1541

Huang, Q., Chen, S., Huang, M. and Guo, Z. (2017), “Adaptive active noise suppression using multiple model switching strategy”, *Shock Vib*. https://doi.org/10.1155/2017/7289076

Kiang, C.T., Spowage, A. and Yoong, C.K. (2015), “Review of control and sensor system of flexible manipulator”, *J. Intel. Robot. Syst.*, **77**(1), 187-213. https://doi.org/10.1007/s10846-014-0071-4

Leniowska, L. and Mazan, D. (2015), “MFC sensors and actuators in active vibration control of the circular plate”, *Arch. Acoust.*, **40**(2), 257-265. https://doi.org/10.1515/aoa-2015-0028

Leva, A. and Piroddi, L. (2011), “FPGA-based implementation of high-speed active noise and vibration controllers”, *Control Eng. Practice*, **19**(8), 798-808. https://doi.org/10.1016/j.conengprac.2011.04.006

Li, Y.P., Lee, T.S. and Wu, B.F. (2014), “A variable step-size sign algorithm for channel estimation”, *Signal Processing*, **102**, 304-312. https://doi.org/10.1016/j.sigpro.2014.03.030

Ma, C., Zhang, X., Xie, S. and Luo, Y. (2015), “Active linear quadratic Gaussian control of the vibration of a flexible beam with a time-varying mass”, *Proceedings of the Institution of Mechanical Engineers, Part I: Journal of Systems and Control Engineering*, **229**(6), 475-484. https://doi.org/10.1177/0959651815573898

Morgan, D.R. (2013), “History, applications, and subsequent development of the FXLMS Algorithm [DSP History]”, *IEEE Signal Process. Magaz.*, **30**(3), 172-176. https://doi.org/10.1109/MSP.2013.2242394

Niu, W., Zou, C., Li, B. and Wang, W. (2019), “Adaptive vibration suppression of time-varying structures with enhanced FxLMS algorithm”, *Mech. Syst. Signal Process.*, **118**, 93-107. https://doi.org/10.1016/j.ymssp.2018.08.009

Pandey, A. and Arockiarajan, A. (2017), “Fatigue study on the sensor performance of macro fiber composite (MFC): Theoretical and experimental approach”, *Compos. Struct.*, **174**, 301-318. https://doi.org/10.1016/j.compstruct.2017.04.066

Pu, Y., Zhou, H. and Meng, Z. (2019), “Multi-channel adaptive active vibration control of piezoelectric smart plate with online secondary path modelling using PZT patches”, *Mech. Syst. Signal Process.*, **120**, 166-179. https://doi.org/10.1016/j.ymssp.2018.10.019

Song, G., Sethi, V. and Li, H.N. (2006), “Vibration control of civil structures using piezoceramic smart materials: A review”, *Eng. Struct.*, **28**(11), 1513-1524. https://doi.org/10.1016/j.engstruct.2006.02.002

Tu, J., Zhang, J., Zhu, Q., Liu, F. and Luo, W. (2018), “The actuation equation of macro-fiber composite coupled plate and its active control over the vibration of plate and shell”, *Struct. Monitor. Mainten.*, **5**(2), 297-311. https://doi.org/10.12989/smm.2018.5.2.297

Zhang, S.Q., Chen, M., Zhao, G.Z., Wang, Z.X., Schmidt, R. and Qin, X.S. (2017), "Modeling techniques for active shape and vibration control of macro-fiber composite laminated structures", *Smart Struct. Syst., Int. J.*, **19**(6), 633-641. https://doi.org/10.12989/sss.2017.19.6.633

Zhao, J., Xu, J., Lo, X.D. and Tian, J. (2007), "An adaptive active noise control algorithm using multiple models", *J. Vib. Eng.*, **20**(6), 549-555. https://doi.org/doi:10.3969/j.issn.1004-4523.2007.06.001

Zhao, Z.L., Qiu, Z.C. and Zhang, X.M. (2016), "Vibration control of a pneumatic driven piezoelectric flexible manipulator using self-organizing map based multiple models", *Mech. Syst. Signal Process.*, **70**, 345-372. https://doi.org/10.1016/j.ymssp.2015.09.041

CC